



## A hybrid decision support system for automatic detection of Schizophrenia using EEG signals

Smith K. Khare, Varun Bajaj\*

*Electronics and Communication Discipline, Indian Institute of Information Technology Design and Manufacturing, Jabalpur, MP, 482005, India*



### ARTICLE INFO

**Keywords:**  
 Schizophrenia  
 Electroencephalography  
 Optimization  
 Robust variational mode decomposition  
 Optimized extreme learning machine classifier

### ABSTRACT

**Background:** Schizophrenia (SCZ) is a serious neurological condition in which people suffer with distorted perception of reality. SCZ may result in a combination of delusions, hallucinations, disordered thinking, and behavior. This causes permanent disability and hampers routine functioning. Trained neurologists use interviewing and visual inspection techniques for the detection and diagnosis of SCZ. These techniques are manual, time-consuming, subjective, and error-prone. Therefore, there is a need to develop an automatic model for SCZ classification. The aim of this study is to develop an automated SCZ classification model using electroencephalogram (EEG) signals. The EEG signals can capture the changes in neural dynamics of human cognition during SCZ.

**Method:** Based on the nature of the SCZ condition, the EEG signals must be examined. For accurate interpretation of EEG signals during SCZ, an automated model integrating a robust variational mode decomposition (RVMD) and an optimized extreme learning machine (OELM) classifier is developed. Traditional VMD suffers from noisy mode generation, mode duplication, under segmentation, and mode discarding. These problems are suppressed in RVMD by automating the selection of quadratic penalty factor ( $\alpha$ ) and a number of modes ( $L$ ). The hyperparameters (HPM) of the OELM classifier are automatically selected to ensure maximum accuracy for each mode without overfitting or underfitting. For the selection of  $\alpha$  and  $L$  in RVMD and HPM in the OELM classifier, a whale optimization algorithm is used. The root mean square error is minimized for RVMD and classification accuracy of each mode is maximized for the OELM classifier. The EEG signals of three conditions performing basic sensory tasks have been analyzed to detect SCZ.

**Results:** The Kruskal Wallis test is used to select different features extracted from the modes produced by RVMD. An OELM classifier is tested using a ten-fold cross-validation technique. An accuracy, precision, specificity, F-1 measure, sensitivity, and Cohen's Kappa of 92.93%, 93.94%, 91.06%, 94.07%, 97.15%, and 85.32% are obtained.

**Conclusion:** The third mode's chaotic features helped to capture the significant changes that occurred during the SCZ state. The findings of the RVMD-OELM-based hybrid decision support system can help neuro-experts for the accurate identification of SCZ in real-time scenarios.

### 1. Introduction

Schizophrenia (SCZ) is a severe mental and chronic illness affecting a person's behavior, feeling, and thinking. According to the World Health Organization (WHO) figures, SCZ affects 20 million people globally [1]. People in their late teens to early thirties are the most likely to be diagnosed with SCZ. Males (early 20s – late adolescent) are more likely than females (early 20s – early 30s) to develop SCZ. It is mainly characterized by three symptoms: negative symptoms, cognitive dysfunction, and positive symptoms. The cognitive dysfunction includes

attention, lack of motivation (unable to perform daily activities), trouble with thinking (deviate from one subject to other with no logical reason), and language. The positive symptoms are confused speech (difficult to understand for others), delusions (false belief not based on reality), and hallucinations (hearing voices and seeing things that don't exist) while the negative symptoms are abnormal memory and reduced will [2,3]. The epidemiological characteristics of SCZ have "three highs (heavy disease burden, disability rate, and recurrence rate) and three lows (compliance, visit rate, and detection)". This may cause damage to different brain tissues and mental decline causing serious mental

\* Corresponding author.

E-mail address: [varunb@iiitdmj.ac.in](mailto:varunb@iiitdmj.ac.in) (V. Bajaj).

disability. As a result, SCZ leads to a declination of occupational and educational performances. The death probability in SCZ is two-three times higher than the healthy population due to physical preventable diseases like a metabolic disease, cardiovascular disorder, and infections. The mortality rate of SCZ patients due to suicide is about 4–6%, the SCZ patients attempt suicide as high as 50% while 13% of the suicidal deaths can be attributed to SCZ [4,5]. The increased disability rate, death rate, and suicide rate in SCZ are due to delayed treatment and/or misdiagnosis of patients. According to the WHO, the treatment of SCZ causes a huge burden on families and healthcare systems [1]. Therefore, there is a need for timely and accurate detection of SCZ from normal healthy control (NHC) subjects to provide ease in an effective diagnosis. Over the past decades, various techniques have been evolved for the detection and diagnosis of SCZ such as interview by experts, medical imaging (e.g. computed tomography, diffusion tensor imaging, magnetic resonance spectroscopy, magnetic resonance imaging), and electroencephalogram (EEG) techniques. Interview by experts are subjective and highly prone to manual errors [6]. Medical-imaging techniques are radio-active, require additional recording, and costly resulting in increased complexity and computational time [2]. One can avoid the above interviewing and medical imaging problems by developing an effective classification model for SCZ using EEG signals. The EEG has effectively detected changes in brain functions, structures, and interaction between neurotransmitters, which has attracted the attention of neurologists, researchers, and other experts [7–10]. Additionally, recording of EEG offers a non-radioactive, low-cost, non-invasive, and portable solution compared to medical-imaging techniques, which motivates us to use EEG for the classification of SCZ.

## 2. Literature review

Various EEG-based studies have been proposed for the detection of SCZ. The average cross mutual information has been measured between in cortical areas of SCZ and NHC to study the changes in EEG signals of different brain regions [11]. Event-related potential (ERP) features have been selected using Wilcoxon rank-sum method and classified with linear discriminant analysis (LDA) classifier in Ref. [6]. A study of ERP and physical features have been explored to detect SCZ using a random forest (RF) classifier [12]. Adaptive boosting and LDA classifiers have been used to classify nonlinear features (Higuchi fractal dimensions, Lampel-Ziv complexity, and entropy) generated directly from EEG signals [13]. In Ref. [14], rhythmic analysis of four frequency bands has been done using filtering and classified with artificial neural networks classifier. The dominant channel selected by mutual information and features extracted using band-power, auto-regressive models, and fractal dimension have been classified with boosting and LDA classifiers [15]. A sensor-level and source-level features have been extracted from filtered EEG signals and classified with a support vector machine (SVM) classifier [16]. A multi-set canonical correlation analysis (MCCA) combining three types of features namely SVM with recursive feature elimination (SVM-RFE), MCCA, and two-sample *t*-test has been used in Ref. [17]. In Ref. [18], filtering, time-frequency representation using Stockwell transform, and k-nearest neighbor (*kNN*) classification have been presented for the SCZ detection.

Rhythm-based effective brain connectivity model comprising of deep neural network and deep belief network (DNN-DBN) have been investigated to classify SCZ and NHC subjects [19]. A study of power spectral densities (PSD) obtained from short-time Fourier transform (STFT) have been explored. The Shannon spectral entropy and median frequency features have been computed to find the discrimination ability of SCZ and NHC using statistical analysis [20]. The wavelet-based decomposition, statistical principal component analysis (S-PCA), and *kNN* classifier have been explored for SCZ classification [21]. A combination of the wavelet transform, Welch PSD, and statistical analysis has been analyzed to find the significant differences between SCZ and NHC subjects [22]. The features extracted from the instantaneous mode functions

(IMF) using empirical mode decomposition (EMD) have been classified with several machine learning techniques (MLT) [23]. Multivariate EMD (M-EMD), entropy features, and different MLT have been evaluated to detect SCZ [24]. A convolutional neural network (CNN) with eleven layers has been used for feature extraction and classification [2]. L1 norm features have been extracted from the wavelet transform decomposed subbands of EEG signals and classified with various MLT [25]. An empirical wavelet transform (EWT) has been used to obtain the features from amplitude and frequency modulated components with MLT [26].

The two-dimensional phase space dynamic of EEG signals plotted on Cartesian space has been presented to extract fifteen graphical features and classified using eight MLT [27]. The study of P300 ERP performing a visual continuous performance task has been explored to detect changes in NHC and SCZ subjects [28]. In Ref. [29], three auditory oddball paradigms have been investigated using multivariate pattern analysis to classify images generated through statistical parametric mapping of spatiotemporal EEG using an SVM classifier. Three conditions of motor-auditory tasks have been analyzed and classified using smoothed pseudo-Wigner Ville distribution and CNN model [30]. The study of amplitude and latency of the P50 and N100 components from auditory evoked responses has been analyzed using iterative independent component analysis to extract statistical features [31]. A mixed model and data-driven classification approach have been presented for the detection of SCZ by investigating relevant ERP features and MLT [32]. The DNN model based on extraction of frequency-domain and time-domain data as a feature has been presented in Ref. [3]. The hybrid DNN model has been designed to classify time-domain and frequency-domain features of EEG signal [33]. The study of EEG rhythms using an autoregressive model and RF classifier has been used to detect SCZ [34]. The study of non-linear and time-domain features has been explored using long short-term memory (LSTM) network for automatic detection of SCZ [35]. A tunable Q wavelet transform (TQWT) has been studied to extract various non-linear features and classified them with the *kNN* classifier [36].

The methods based on direct analysis of EEG signals may not provide representative information while the fast Fourier transform (FFT)-based approach results in localization problems of time-frequency. The STFT requires a fixed-length window and assumes the signal to be stationary. The fractal-dimension algorithms are noise-prone while EMD-based analysis suffers mathematical modeling. The wavelet-based decomposition methods are required to provide a type of wavelet, TQWT-based decomposition requires a choice of tuning parameter for decomposing signal into subbands, and deep learning-based CNN requires higher memory and computational time. Moreover, the use of fixed and empirical parameter setups offers no representative information for the study of spontaneously varying EEG signals and contributes to restricted system performances (e.g. accuracy, sensitivity, specificity). This encourages us to develop a robust variation mode decomposition (RVMD) and an optimized extreme learning machine (OELM) classifier for the automatic classification of SCZ. RVMD selects the decomposition parameters (quadratic penalty factor and number of modes) automatically in accordance with the varying nature of EEG signals. The OELM classifier uses an automatic selection of hyperparameters (hidden neurons, kernel function, and weight calculator) to maximize the accuracy by regulating the overfitting and underfitting problem. A combination of optimum value based variational mode decomposition (VMD) and different MLT has been proven effective in various physiological problems such as motor imagery task detection, drowsiness, and emotion classification [37–39].

The proposed approach uses EEG signal analysis based on Kaggle's basic sensory task data. Analysis and synthesis of EEG signals are performed using RVMD. The statistical measures computed from informative modes are fed to the OELM classifier. The system model is evaluated by measuring various performance measures and comparing them with current state-of-the-art (C-SOA) techniques. The remainder of this paper is structured as: Section 3 provides an overview of materials and

methods, Section 4 presents the results, Section 5 provides a performance comparison with C-SOA, and Section 6 summarizes the conclusions.

### 3. Materials and methods

The proposed method involves data-source as EEG signals, analysis and synthesis using RVMD, features as statistical measures, and classification of NHC and SCZ using OELM classifier. The steps of the proposed hybrid decision support system (HDSS) are illustrated in Fig. 1.

#### 3.1. Data-set

The open-source EEG data-set of SCZ downloaded from Kaggle is used in this study [40,41]. The EEG recordings have been acquired from 8 external and 64 scalp sites. A total of 81 (14 female and 67 male) participants were used for acquisition, including 49 (8 female and 41 male) SCZ patients and 32 (6 female and 26 male) NHC subjects. The mean age of SCZ and NHC subjects was  $40.02 \pm 13.55$  and  $38.37 \pm 13.69$  years while the mean level of education was  $13.55 \pm 1.65$  and  $15.92 \pm 1.95$ , respectively. A simple push-button task was used in which subjects either (i) pressed a button to immediately generated a tone, (ii) passively listened to the same tone, or (iii) pressed a button without generating a tone to study the corollary discharge in people with SCZ and comparison controls. These three tasks are identified as three conditions (C-I, C-II, and C-III). EEG recordings were continuously digitized at 1024 Hz and referenced off-line to averaged earlobe electrodes.

The data from each subject were pre-processed as (a) highpass filter at 0.1 Hz, (b) interpolation of outlier channels in the continuous EEG data, (c) a continuous data chopped into single-trial epochs 1.5 s before and after the tasks (3 s total), (d) baseline corrections –100 to 0 ms, (e) high-frequency white noise and muscle artifacts were removed using

canonical correlation analysis, (f) rejection of outlier single trials, (g) removal of outlier components from a spatial ICA, and (h) interpolation of outlier channels within single trials. Each trial consists of 3072 sample points and a total number of signals analyzed for each condition (NHC and SCZ) is (i) 3108 and 4608, (ii) 3015 and 4506, and (iii) 3111 and 4520, respectively. Typical EEG signals of NHC and SCZ subjects for each condition are shown in Fig. 2.

#### 3.2. Robust variational mode decomposition

VMD divides a signal into modes having specific sparsity property [42]. The decomposition of a signal into multiple modes is controlled by the quadratic penalty factor and the number of modes. Improper selection of  $L$  and  $\alpha$  can produce higher decomposition error and loss of information. Selection of too large or too small values of  $L$  and  $\alpha$  may incur the following conditions [42]:

- Under segmentation of data as some components may occur in other modes (Small  $L$  and  $\alpha$ ).
- Discarding some modes as a noise (Small  $L$  and large  $\alpha$ ).
- Capturing the extra noise (Large  $L$  and small  $\alpha$ ).
- Mode duplication (Large  $L$  and  $\alpha$ ).

To avoid these conditions, a precise selection of  $L$  and  $\alpha$  is required for proper analysis and synthesis of EEG signals. The adaptive selection of a number of modes by evaluating the permutation entropy and kurtosis has been explored in Ref. [43]. It uses an empiric selection of threshold to select a number of modes. As EEG signals are considered as low amplitude, this threshold may be too high. Also, it does not consider the quadratic penalty factor  $\alpha$  which greatly affects the decomposition error. Automatic selection of  $L$  and  $\alpha$  have been explored based on dynamic entropy and power spectral entropy [44]. These methods are

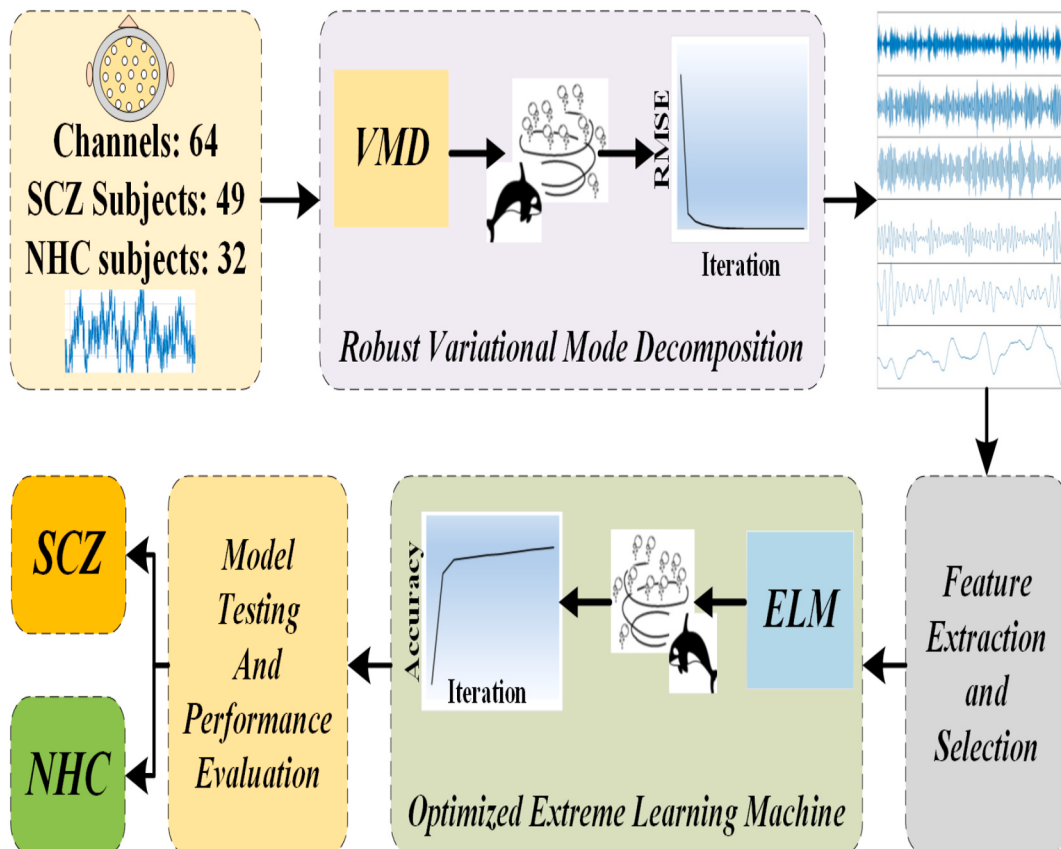
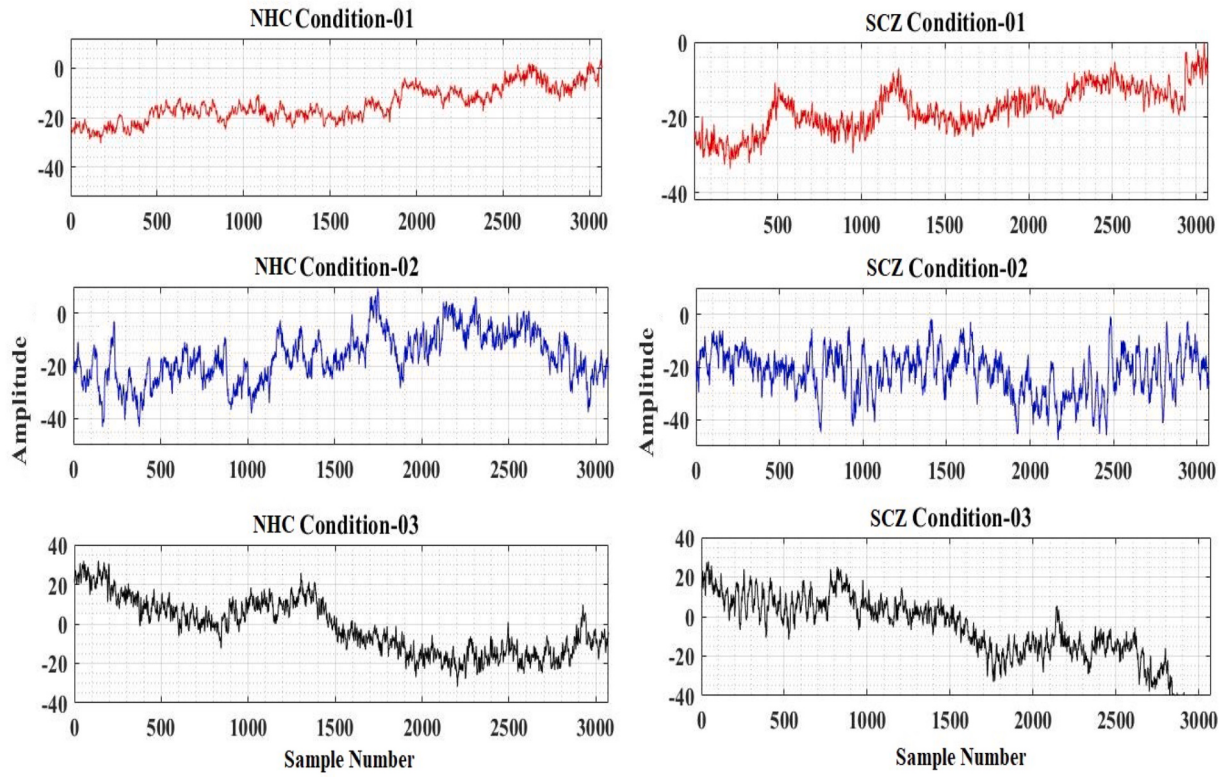


Fig. 1. Proposed HDSS model for the classification of SCZ.



**Fig. 2.** Examples of EEG signals at various conditions: (a) NHC, and (b) SCZ.

based on features for adaptive selection of parameters. To overcome this, RVMD is proposed for self-selection of  $L$  and  $\alpha$  depending on the nature of EEG signals. The method presented in this paper does not involve the prior evaluation of features to decide the values of  $L$  and  $\alpha$ . For each mode, the frequency shift is applied with respect to central frequency. The spectral property of spectral-domain bandwidth is chosen. Squared  $\mathcal{L}_2$  norm of the gradient is used for estimating the bandwidth to model constrained optimization problem as [42].

$$\min_{\{\widehat{v}_l\}, \{\widehat{w}_l\}} \sum_l \left\| \partial_t \left[ \left( \delta(t) + \frac{j}{\pi t} \right) * \widehat{v}_l(t) \right] e^{-j\widehat{w}_l t} \right\|_2^2 \quad \text{and} \quad \sum_l \widehat{v}_l = z \quad (1)$$

Constrained problem is converted to unconstrained one with the help of Langrangian multiplier  $\widehat{\lambda}$  and quadratic penalty factor  $\alpha$  denoted as [42].

$$\mathcal{L}\left(\{\widehat{v}_l\}, \{\widehat{w}_l\}, \widehat{\lambda}\right) = \alpha \sum_l \left\| \partial_t \left[ \left( \delta(t) + \frac{j}{\pi t} \right) * \widehat{v}_l(t) \right] e^{-j\widehat{w}_l t} \right\|_2^2 + \left\| z(t) - \sum_l \widehat{v}_l(t) + \frac{\widehat{\lambda}(t)}{2} \right\|_2^2 + \langle \widehat{\lambda}(t), z(t) - \sum_l \widehat{v}_l(t) \rangle \quad (2)$$

The minimization w.r.t  $\widehat{v}_l$  is rewritten as [42]:

$$\widehat{v}_l^{n+1} = \arg \min_{\widehat{v}_l \in X} \left\{ \alpha \left\| \partial_t \left[ \left( \delta(t) + \frac{j}{\pi t} \right) * \widehat{v}_l(t) \right] e^{-j\widehat{w}_l t} \right\|_2^2 + \left\| z(t) - \sum_l \widehat{v}_l(t) + \frac{\widehat{\lambda}(t)}{2} \right\|_2^2 \right\} \quad (3)$$

The minimization w.r.t  $\widehat{w}_l$  is expressed by Ref. [42]:

$$\widehat{w}_l^{n+1} = \arg \min_{\widehat{w}_l} \left\{ \left\| \partial_t \left[ \left( \delta(t) + \frac{j}{\pi t} \right) * \widehat{v}_l(t) \right] e^{-j\widehat{w}_l t} \right\|_2^2 \right\} \quad (4)$$

A signal decomposed into multiple modes using VMD can be denoted by

$$z(t) = z_a(t) + e_d(t) \quad (5)$$

where  $z(t)$  is the original signal,  $z_a(t)$  is the approximated signal, and  $e_d(t)$  is the error of decomposition. To minimize  $e_d(t)$ , a precise selection of  $L$  and  $\alpha$  is required which is laborious and time-consuming. Hence, an optimization technique is employed for automating the  $L$  and  $\alpha$ . The cost function of root mean square error (RMSE) is used as a constraint of RVMD expressed by

$$rmse_d = \sqrt{\frac{1}{T} \sum_t^T (z(t) - z_a(t))^2} \quad (6)$$

where  $rmse_d$  is root mean square error of decomposition. To formulate the problem, this method minimizes  $rmse_d$  represented by

$$CF = \min(rmse_d) \quad (7)$$

The signal  $z_a(t)$  is mathematically expressed as  $\sum_{l=1}^L \widehat{v}_l(t)$ , where  $\widehat{v}_l$  is the  $l$ th mode. The minimization of the above-defined constraint and

optimal solution is obtained by the whale optimization algorithm (WOA). The whales are the biggest mammal on the globe and considered to be highly intelligent [45]. Whales are mostly predators having their favorite prey like small fish herds and krill. The humpback whales use a special hunting method called bubble-net feeding. WOA is inspired by the hunting technique of this humpback whale. WOA is accomplished in three steps namely searching, encirclement, and bubble-net attacking method. The search for prey is expressed as [45]:

$$\begin{aligned} \tilde{O} &= \left| \tilde{C} \cdot \tilde{S}_r - \tilde{S}_w \right| \\ \tilde{S}_w(i+1) &= \tilde{S}_r - \tilde{D} \cdot \tilde{O} \end{aligned} \quad (8)$$

The encirclement is governed by Ref. [45]:

$$\begin{aligned} \tilde{O} &= \left| \tilde{C} \cdot \tilde{S}_b(i) - \tilde{S}_w(i) \right| \\ \tilde{S}_w(i+1) &= \tilde{S}_b(i) - \tilde{D} \cdot \tilde{O} \end{aligned} \quad (9)$$

The whales simultaneously swim around the prey along a spiral-shaped path and within a shrinking circle. This shrinking and encircling or spiral mechanism for position updation is assumed with a probability ( $p$ ) of 50%. The bubble net attacking module is represented by [45].

$$\tilde{S}_w(i+1) = \begin{cases} \tilde{S}_b(i) - \tilde{D} \cdot \tilde{O}, p < 0.5 \\ \tilde{O}^l \cdot e^{bl} \cdot \cos(2\pi l) + \tilde{S}_b(i), p \geq 0.5 \end{cases} \quad (10)$$

The coefficient vectors  $\tilde{C}$  and  $\tilde{D}$  are defined as [45]:

$$\begin{aligned} \tilde{D} &= 2a \cdot r - a \\ C &= 2 \cdot r \end{aligned} \quad (11)$$

where  $\tilde{S}_b$  is the best solution obtained so far,  $\tilde{S}_r$  is the random position vector of random whale, and  $\tilde{S}_w$  is the position vector.  $\tilde{O}$  denotes the encirclement vector. The vectors  $\tilde{D}$  and  $\tilde{C}$  denote coefficient vectors. The vector  $O^l = |\tilde{S}_b(i) - \tilde{S}_w(i)|$  indicates the distance between  $i$ th whale to prey. The shape of logarithmic spiral is defined by constant  $b$ ,  $l$  is the random number in the range [-1,1],  $r$  is the random vector in the range [0,1],  $a$  decreases linearly from 2 to 0 with advancement in the iteration,  $i$  is the iteration, “||” denotes absolute value, and “.” represents element-by-element multiplication. The optimum modes ( $L_{opt}$ ) obtained for each signal of two classes are different. Therefore, to maintain the synchronization between each condition and class, a minimal number of modes ( $L_{minimal}$ ) are evaluated and represented as

$$L_{minimal} = \text{floor} \left( \frac{1}{P} \frac{1}{Q} \frac{1}{R} \sum_{p=1}^P \sum_{q=1}^Q \sum_{r=1}^R L_{opt}^{pqr} \right) \quad (12)$$

The typical modes obtained from RVMD is shown in Fig. 3.

### 3.3. Features

Six features namely log detector (LogD), Tsallis entropy (TsEn), the absolute value of fifth temporal moment (TMF), Shannon entropy (ShEn), interquartile range (IQR), and Renyi's entropy (ReEn) are given to the classifier. The mathematical formulation of these features are represented by Refs. [37,46]:

$$\begin{aligned} TMF &= \left| \frac{1}{T} \sum_{t=1}^T \hat{v}_t^5 \right| \\ LogD &= e^{\frac{1}{T} \sum_{t=1}^T \log |\hat{v}_t|} \\ IQR &= Q_3 - Q_1 \\ ReEn &= \frac{1}{1-\gamma} \left( \log \sum_{t=1}^T p_i(\hat{v}_t)^\gamma \right) \\ ShEn &= - \sum_{t=1}^T p_i(\hat{v}_t) \cdot \log p_i(\hat{v}_t) \\ TsEn &= \frac{1 - \sum_{t=1}^T p_i(\hat{v}_t)^r}{r-1} \end{aligned} \quad (13)$$

where  $T$  is the length of EEG signal.  $Q_1$  is first quartile,  $Q_3$  is third quartile, and  $p_i$  is the probability of occurrence. The constant  $\gamma$  and  $r$  is taken as 2.

### 3.4. Optimized extreme learning machine classifier

A feedforward single-layer neural network called ELM classifier has the ability to classify binary and multi-label information [47]. It is required to set the number of hidden neurons during the training and testing of the ELM classifier. The assignment of hidden layer bias weights and the weight between input and hidden layers are done randomly. To obtain final weights for hidden and output layers, the least-square criteria and the Moore-Penrose pseudo-inverse method are used. The activation function for  $Z$  hidden points and a set of  $M$  distinct input such that  $\{p_1, p_2, \dots, p_M, c_1, c_2, \dots, c_M\}$  is denoted by Ref. [47]:

$$\sum_{k=1}^Z \beta_k h_k(p_j) = \sum_{k=1}^Z \beta_k h_k(b_k \cdot p_j + d_k) = c_j \quad (14)$$

where  $b_k = [b_{k1}, b_{k2}, \dots, b_{kM}]^T$  is the weight vector between predictor and hidden nodes,  $\beta_k = [\beta_{k1}, \beta_{k2}, \dots, \beta_{kM}]^T$  is weight vector joining hidden and target nodes,  $d_k$  is threshold,  $b_k \cdot p_j$  is the inner product of  $b_k$  and  $p_j$ . The conversion of target matrix to least squares and its corresponding solution is defined as [47].

$$\begin{aligned} H\beta &= M \\ \|H(b_1, \dots, b_Z, d_1, \dots, d_Z)\hat{\beta} - M\| &= \\ \min_{\beta} \|H(b_1, \dots, b_Z, d_1, \dots, d_Z)\hat{\beta} - M\| \\ \hat{\beta} &= H^{\dagger} M \end{aligned} \quad (15)$$

where  $\hat{\beta}$  is an optimal solution and  $H^{\dagger}$  is Moore-Penrose. The selection of appropriate kernel (AK), weight calculator function (WCF), and a number of hidden neurons (HN) are required as hyperparameters (HPM) of the ELM classifier. An experimental and random selection of HPM may increase misclassification. The manual selection of correct HPM is time-consuming, prone to error, and exhaustive. For the selection of optimized and accurate HPM, OELM classifier is proposed. The WOA is used for automatic selection of AK, HN, and WCF in OELM classifier. A cost function of maximum accuracy (ACC) is chosen and represented as

$$\begin{aligned} ACC &= \frac{T_p + T_n}{T_p + F_p + T_n + F_n} \\ CF &= \max(ACC) \end{aligned} \quad (16)$$

where  $T_p$  is true positive,  $F_n$  is false negative,  $T_n$  is true negative, and  $F_p$  is false positive instances. The pseudo-code for the proposed HDSS is shown in Algorithm 1.

**Algorithm 1.** Pseudo-code of HDSS model.

**Algorithm 1** Pseudo-code of HDSS model.

---

1: Randomly set the initial values of  $L$  and  $\alpha$ .

2: Obtain the modes by decomposing EEG signal with RVMD.

3: Compute the approximated signal  $z_a(t) = \sum_{l=1}^L \hat{v}_l$ .

4: Compute the root mean square decomposition error ( $rmse_d$ ) as  $\sqrt{\frac{1}{T} \sum_t^T (z(t) - z_a(t))^2}$ .

5: **while** ( $min(rmse_d)$ ) **do**

6:   **if** ( $rmse_d == min$ ) **then**

7:     The quadratic penalty factor and number of modes are optimum.

8:   **else**

9:     Repeat the steps (1-8) for different values of  $L$  and  $\alpha$ .

10:   **end if**

11: **end while**

12: Use  $L_{opt}$  and  $\alpha_{opt}$  with  $min(rmse_d)$ .

13: Compute minimal value of mode using the relation  $L_{minimal} = floor\left(\frac{1}{P} \frac{1}{Q} \frac{1}{R} \sum_{p=1}^P \sum_{q=1}^Q \sum_{r=1}^R L_{opt}^{pqr}\right)$ .

14: Decompose the signals with  $L_{minimal}$  and  $\alpha_{opt}$ .

15: Evaluate different linear and non-linear features from each mode.

16: Select the best discriminant features using the KW test.

17: Feed input feature matrix of each mode to OELM classifier.

18: Set AK, HN, and WCF randomly.

19: Compute the  $ACC$  with initial AK, HN, and WCF using Eq. (16).

20: **while** ( $max(ACC)$ ) **do**

21:   **if** ( $ACC == max$ ) **then**

22:     The AK, WCF, and HN are optimum.

23:   **else**

24:     Repeat the steps (17-23) for each mode with different combination of AK, HN, and WCF.

25:   **end if**

26: **end while**

27: Evaluate performance parameters using optimum combination of HN, AK, and WCF having  $max(ACC)$ .

---

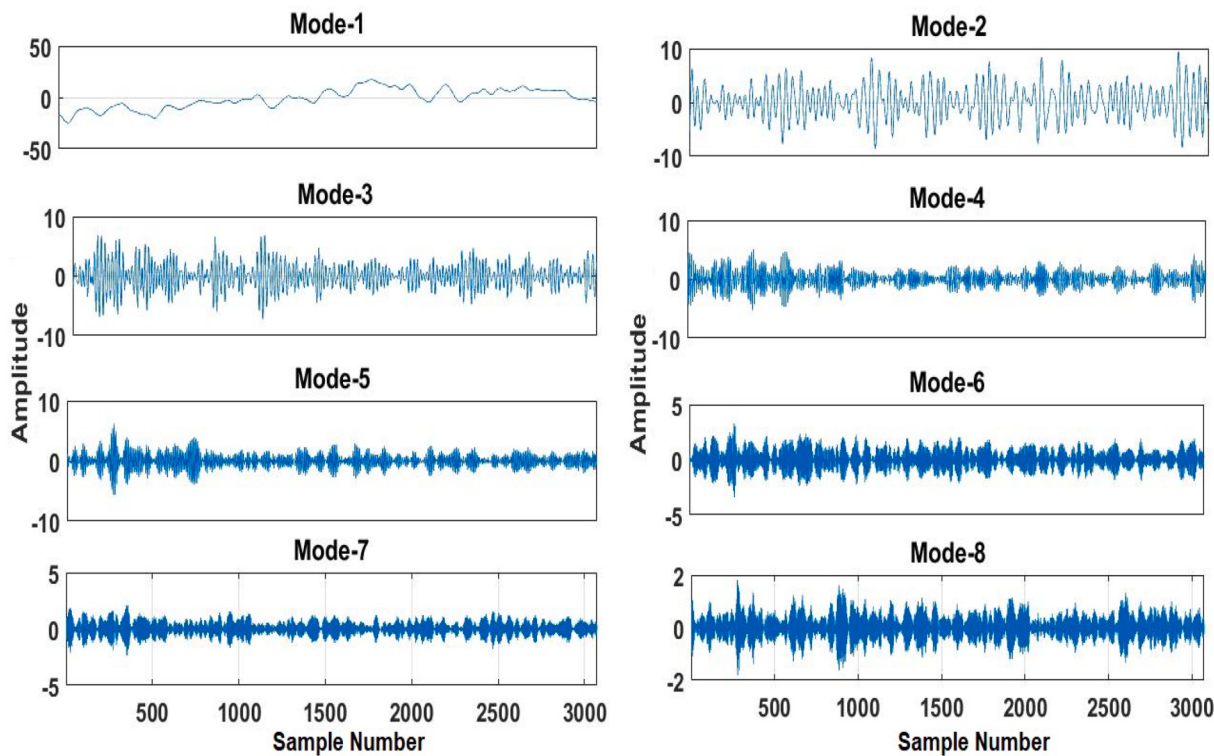


Fig. 3. Typical modes extracted using RVMD.

#### 4. Results

The proposed HDSS is evaluated for signal analysis by computing an accuracy using the OELM classifier and synthesis by minimizing the reconstruction error of the recovered signal. The discrimination ability of SCZ and NHC signals is evaluated by analyzing three conditions of basic push-button tasks. The common experimentation platform is maintained to evaluate the developed technique. The noise tolerance is kept  $10^{-5}$ , omegas are initialized uniformly, and no DC part is imposed for both RVMD and VMD. The number of modes and penalty factor are empirically set to 4 and 2500, respectively for VMD. The search agents and maximum iterations are set as 30 and 50 for WOA. The RMSE obtained using RVMD and VMD for three conditions are shown in Table 1. It is noticed from Table 1, RVMD provides a better synthesis of EEG signals over VMD for SCZ and NHC classes. The error provided by RVMD is 100 times less compared to traditional VMD.

The findings of Table 1 motivates us to use the optimal parameters of RVMD provided by WOA for adaptively decomposing EEG signals. A minimal number of modes are computed using Eq. (12) to maintain the uniformity in each condition and obtained as 8. The Kruskal Wallis (KW) test is used to investigate the statistical properties of features. Table 2 indicates the probabilistic chi values obtained for six features. It is seen from Table 2, each feature has probabilistic value less than 0.05.

The matrix of six features is fed to the ELM classifier to compute the ACC of each mode using four kernels (sigmoid (SIG), triangular basis (TB), sine (SIN), and radial basis function (RBF)). A ten-fold cross-validation technique is employed to perform classification in which input is partitioned into ten equal parts. One part is used for testing while nine parts are utilized for training. The ACC for each mode of VMD and RVMD using four kernels of ELM classifier are shown in Tables 3 and 4. The highest ACC of 81.67% is provided by C-I in mode three (P-3) of RBF kernel. The highest ACC of 68.86% is obtained for C-III while the

least of 68.04% is obtained for C-II using VMD and ELM classifier. The ACC provided by RVMD using ELM classifier is maximum for RBF kernel with 90.77% in C-I while it is 64.30% and 67.04% in conditions II and III. It is evident from Tables 3 and 4, the developed RVMD model has generated informative modes over traditional VMD.

The OELM classifier is used for an automatic selection of HPM. The features extracted from the modes of VMD and RVMD are classified using the OELM classifier. The accuracies obtained for each mode of VMD and RVMD using the OELM classifier are shown in Tables 5 and 6. The highest ACC obtained using VMD and OELM classifier for C-I, C-II, and C-III is 83.16%, 69.02%, and 69.37%, respectively. On the other hand, the highest ACC obtained for C-I, C-II, and C-III using modes of RVMD and OELM classifier is 92.93%, 69.59%, and 70.12% in P-3 and P-2. It is noticed from Tables 3–6, the ACC provided by RVMD using the OELM classifier is superior to VMD for all three conditions. The modes generated using RVMD and the best combination of HPM provided by the OELM classifier showed better analysis and the highest classification of EEG signals. The variations provided by C-I are highly discriminant in classifying SCZ and NHC EEG signals compared to C-II and C-III, respectively. As C-I achieved the highest ACC, further analysis is done in accordance with it. To get a detailed insight of the proposed HDSS using RVMD and OELM classifier, six performance parameters (sensitivity (SEN), F-1 score (F1), specificity (SPE), ACC, Cohen's Kappa (Kappa), and precision (PrC)) are computed.

As evident from Table 7, P-3 has provided maximum values of SPE, F1, Kappa, PrC, and ACC of 91.06%, 94.07%, 85.32%, 93.94%, and 92.93% while the highest SEN of 97.15% is achieved in P-4, respectively. The mode P-1 has provided the least values of performance measures. The highest performance of the third mode is due to its chaotic properties. The first mode contains very low-frequency components providing the least discrimination ability. The presence of high-frequency contents in higher modes has signal information combined with some noise.

Fig. 4 provides a fold-wise variation of the performance measures in P-3 for C-I. It is evident from the Figure, variation of each performance

**Table 1**  
RMSE obtained using VMD and RVMD for each condition.

Class	Conditions	VMD	RVMD
NHC	C-I	$2.071 \times 10^{-06}$	$2.321 \times 10^{-08}$
	C-II	$2.121 \times 10^{-06}$	$2.436 \times 10^{-08}$
	C-III	$1.958 \times 10^{-06}$	$2.178 \times 10^{-08}$
SCZ	C-I	$1.683 \times 10^{-06}$	$1.724 \times 10^{-08}$
	C-II	$1.713 \times 10^{-06}$	$1.701 \times 10^{-08}$
	C-III	$1.682 \times 10^{-06}$	$1.579 \times 10^{-08}$

**Table 2**  
Probability of chi obtained from KW test.

Mode	LogD	ReEn	TMF	IQR	ShEn	TsEn
P-1	$1.6 \times 10^{-60}$	$2.2 \times 10^{-57}$	$7.4 \times 10^{-34}$	$1 \times 10^{-63}$	$3.7 \times 10^{-38}$	$1.4 \times 10^{-57}$
P-2	$6.3 \times 10^{-04}$	$1.1 \times 10^{-04}$	$2.7 \times 10^{-62}$	$9.1 \times 10^{-04}$	$3.7 \times 10^{-04}$	$1.1 \times 10^{-04}$
P-3	$2.7 \times 10^{-07}$	$3.9 \times 10^{-08}$	$8.1 \times 10^{-08}$	$3.1 \times 10^{-07}$	$9.2 \times 10^{-08}$	$3.9 \times 10^{-08}$
P-4	$5.8 \times 10^{-05}$	$4.1 \times 10^{-05}$	$2.9 \times 10^{-18}$	$9.1 \times 10^{-05}$	$6.1 \times 10^{-05}$	$4.1 \times 10^{-05}$
P-5	$5.9 \times 10^{-06}$	$8.1 \times 10^{-06}$	$9.7 \times 10^{-05}$	$4.8 \times 10^{-06}$	$8.9 \times 10^{-06}$	$8.1 \times 10^{-06}$
P-6	0.037	0.0448	$2.3 \times 10^{-19}$	0.034	0.048	0.049
P-7	$8.7 \times 10^{-05}$	$7.5 \times 10^{-05}$	$4.7 \times 10^{-30}$	$6.4 \times 10^{-05}$	$1.1 \times 10^{-04}$	$7.5 \times 10^{-05}$
P-8	$1.1 \times 10^{-14}$	$3.6 \times 10^{-15}$	$4.1 \times 10^{-65}$	$1.2 \times 10^{-14}$	$8.7 \times 10^{-15}$	$3.6 \times 10^{-15}$

measure is minimal from the mean. This makes our developed HDSS model effective. Table 8 shows the percentage confusion matrix of each class for C-I in P-3 mode. The SCZ class has provided a 93.94% correct classification rate and the NHC class has identified 91.44% of signals correctly.

## 5. Performance comparison

Table 9 presents the comparison report of HDSS with C-SOA techniques. Sabeti et al. [13] used Lampel-Ziv complexity, Higuchi fractal dimensions, and entropy (Shannon, approximate and spectral) analysis. Their method provided an ACC of 90% and 86% for all features. The features selected using a genetic algorithm yielded an ACC of 91% and 89% for boosting and LDA classifiers. Their study showed the

**Table 3**  
Accuracy score obtained for each condition using VMD and ELM classifier (%).

kernel	SIG	SIN	TB	RBF
<b>Condition-I</b>				
P-1	63.49	62.34	62.8	65.14
P-2	72.79	75.16	75.84	75.52
P-3	76.77	80.79	80.84	81.67
P-4	75.47	80.17	79.84	81.04
<b>Condition-II</b>				
P-1	63.29	64.05	64.15	64.43
P-2	66.01	67.4	66.58	67.62
P-3	67.41	67.85	67.83	68.04
P-4	66.3	67.41	67.98	68.02
<b>Condition-III</b>				
P-1	61.73	62.73	59.11	63.15
P-2	65.53	66.73	67.06	68.13
P-3	67.06	68.24	67.62	68.86
P-4	65.01	66.91	68.22	68.22

**Table 4**  
Accuracy score obtained for each condition using RVMD and ELM classifier (%).

Kernel	SIG	SIN	TB	RBF
<b>Condition-I</b>				
P-1	62.97	63.45	63.11	63.54
P-2	87.46	87.22	86.91	88.87
P-3	86.85	88.87	89.64	90.77
P-4	88.86	88.00	89.05	89.64
P-5	86.75	85.78	86.25	86.84
P-6	80.42	80.73	79.47	80.83
P-7	75.56	76.47	75.25	77.41
P-8	74.68	76.99	79.11	79.14
<b>Condition-II</b>				
P-1	60.92	62.11	62.22	60.92
P-2	64.30	65.41	66.16	64.30
P-3	63.46	64.33	64.73	63.46
P-4	61.11	62.25	62.49	61.11
P-5	62.92	63.13	63.32	62.92
P-6	62.17	62.79	62.72	62.17
P-7	61.47	62.10	62.23	61.47
P-8	61.85	62.49	62.41	61.85
<b>Condition-III</b>				
P-1	62.51	63.15	62.75	63.34
P-2	64.88	65.51	67.72	67.21
P-3	64.96	66.07	66.22	67.04
P-4	64.38	64.92	62.65	64.99
P-5	64.30	64.64	62.40	64.48
P-6	63.14	63.69	62.72	63.48
P-7	63.89	64.34	63.35	64.39
P-8	63.68	64.15	62.25	64.36

**Table 5**  
Accuracy score obtained for each condition using VMD and OELM classifier (%).

Modes	C-I	C-II	C-III
P-1	69.52	65.03	62.23
P-2	77.48	68.22	68.78
P-3	83.16	68.86	68.98
P-4	82.96	69.02	69.37

**Table 6**  
Accuracy score obtained for each condition using RVMD and OELM classifier (%).

Modes	C-I	C-II	C-III
P-1	65.73	65.03	64.43
P-2	90.98	69.59	70.12
P-3	92.93	69.33	68.48
P-4	92.46	69.46	66.96
P-5	89.81	68.20	66.00
P-6	83.84	66.58	65.78
P-7	82.08	66.15	65.07
P-8	82.31	67.50	65.28

**Table 7**  
Measure of performance for C-I.

Measure	ACC	SEN	SPE	F1	PrC	Kappa
P-1	65.73	67.22	61.69	74.33	83.18	24.48
P-2	90.99	94.22	86.68	92.29	90.46	81.45
P-3	92.93	94.21	91.06	94.07	93.94	85.32
P-4	92.46	97.15	86.72	93.44	90.03	84.61
P-5	89.81	96.41	82.29	90.97	86.14	79.34
P-6	83.84	93.02	74.49	85.33	78.86	67.60
P-7	82.08	89.33	73.93	84.10	79.49	63.71
P-8	82.31	89.64	74.11	84.28	79.55	64.21

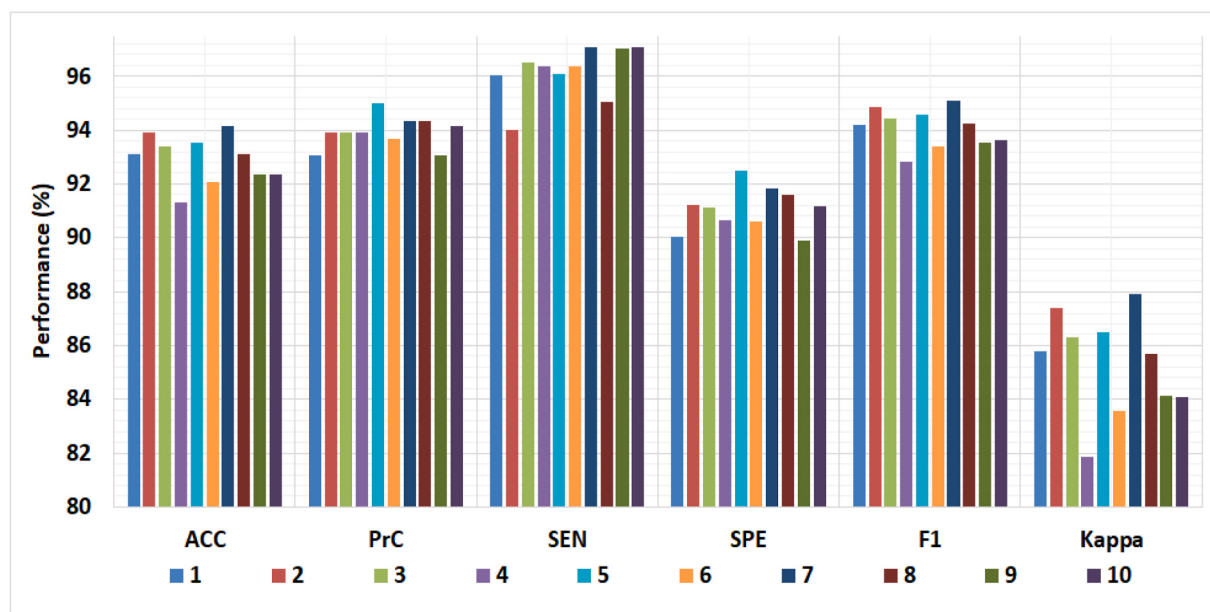


Fig. 4. Foldwise variation of performance measures.

Table 8

Confusion matrix (%) of C-I obtained for mode 3.

Class	SCZ	NHC
SCZ	93.94	6.06
NHC	8.56	91.44

resting-state potential of the limbic region in SCZ has more differentiating information over NHC subjects. Li et al. [14] used rhythm-based analysis using filtering technique. The alpha, beta, theta, and delta rhythms with self-organizing maps (SOM) and backpropagation multi-layer perceptron (BP-MLP) classifiers have obtained an overall ACC in 40–60% and 60–80% range. Sabeti et al. [15] used entropy and mutual information-based channel selection algorithm, followed by feature extraction based on band-power of rhythms, fractal dimensions (Petrosian, Katz, and Higuchi method), and an autoregressive (AR) model coefficients. Features classified directly and selected using a genetic algorithm have obtained an ACC of 85.90% and 91.94%.

The model presented by Aharon et al. [18] combines Stockwell transform, optimal feature selection, and kNN classification technique to develop time-frequency transformation followed by feature-optimization (TFFO) has reported an ACC of 88.7%. Their study showed electrodes located in the frontal region reflect discriminable characteristics for SCZ and NHC detection. Shim et al. [16] used auditory oddball task to extract sensor-level (1–30 Hz bandpass filter) and source-level (minimum norm estimation using 1–55 Hz bandpass filter). An SVM classifier has generated the maximum ACC of 80.88%, 85.29%, and 88.24% with ten sensor levels, four source levels, and fifteen combined features. Sui et al. [17] used the MCCA method for feature extraction combining two-stage t-test, SVM-RFE, and MCCA coefficients. The ACC of 70% for SVM-RFE, 66% for two-stage t-test, 69% for MCCA, and 74% for combined features have been obtained using the SVM classifier. Phang et al. [19] used graph-theoretical complex network measures and vector-autoregression-based directed connectivity method to extract different features from the rhythms of EEG signals. The separate and combined features classified using DNN-DBN have achieved an ACC in the range 70%–95%. Krishnan et al. [24] employed M-EMD to extract instantaneous amplitude and frequency components.

Table 9

Comparison of HDSS with C-SOA techniques.

Authors	Dataset	Method	Features	Accuracy
Sabeti et al. [13]	20 SCZ and 20 NHC subjects	Non-linear method & Adaboost	–	91
Li et al. [14]	10 NHC and 10 SCZ subjects	Rhythms & BP-MLP	–	80
Sabeti et al. [15]	20 SCZ and 20 NHC subjects	Non-linear method & Adaboost	100	91.94
Aharon et al. [18]	25 SCZ and 25 NHC subjects	Stockwell transform & kNN	13	88.7
Shim et al. [16]	34 SCZ and 34 NHC subjects	sensor-source level & SVM	438	88.24
Sui et al. [17]	48 SCZ and 53 NHC subjects	ICA & SVM-RFE	–	74
Phang et al. [19]	45 SCZ and 39 NHC subjects	Connectivity feature & DNN-DBN	170	95
Krishnan et al. [24]	14 SCZ and 14 NHC subjects	M-EMD & SVM	20	90
Oh et al. [2]	14 SCZ and 14 NHC subjects	CNN	–	98.07
Devia et al. [6]	11 SCZ and 9 NHC subjects	Bandpass filter & LDA	–	71
Sharma et al. [25]	14 SCZ and 14 NHC subjects	Orthogonal wavelet & kNN	7	99.21
Zhang [12]	49 SCZ and 32 NHC subjects	Pre-processing & RF	8	81.1
Siuly et al. [23]	49 SCZ and 32 NHC subjects	EMD & EBT	5	89.59
Khare et al. [26]	49 SCZ and 32 NHC subjects	EWT & SVM	5	88.7
Akbari et al. [27]	14 SCZ and 14 NHC subjects	Graphical features & kNN	15	94.8
Guo et al. [3]	49 SCZ and 32 NHC subjects	Electrical marker & DNN	21	92
Sun et al. [33]	54 SCZ and 55 NHC subjects	FFT & DNN	–	96.34
Chandran et al. [35]	14 SCZ and 14 NHC subjects	LSTM	6790	99
Baygin [36]	14 SCZ and 14 NHC subjects	TQWT & kNN	25	99.12
<b>Proposed</b>	49 SCZ and 32 NHC subjects	<b>RVMD &amp; OELM</b>	<b>6</b>	<b>92.93</b>

Different entropy features selected with RFE and classified using the RBF kernel of the SVM classifier yielded an accuracy of 90% with a reduced 20 feature set. Oh et al. [2] obtained an ACC of 98.07% and 81.26% for non-subject and subject-based automatic feature extraction and classification of EEG signals using an 11-layered CNN model. The model explored by Devia et al. [6] used ERP features of frontal, central, parietal, and occipital regions. Their model showed occipital region plays a key role in discriminating SCZ and NHC with an ACC of 71% using the LDA classifier. Sharma and Acharya [25] used six levels of optimal two-band orthogonal wavelet filter bank called RMSFSM to extract L1 norm features. Their method provided an ACC of 99.21% and 97.2% using *kNN* classifier with ten-fold and leave-one-subject-out cross-validations.

Zhang [12] used ERP, age, education, and conditional features to separate SCZ and NHC subjects. The combination of these features has obtained an ACC of 81.1% using an RF classifier. Their study showed ACC improves with an increase in the number of features. Siuly et al. [23] investigated an EMD-based decomposition to extract IMFs. Five features extracted from IMFs and selected using the KW test have achieved an ACC of 89.59% for the second IMF using an ensemble bagged tree (EBT) classifier. The method presented by Khare et al. [26] combined EWT, feature extraction, and classification with various MLT. Their model yielded an ACC score of 88.7% for the first band with five features and an SVM classifier. Akbari et al. [27] used two-dimensional phase space dynamic to study the chaotic behavior of fifteen features. A forward selection algorithm used for the relevant features has obtained an ACC of 94.8% using the *kNN* classifier. Their model showed parietal and frontal lobe provides a better representation of SCZ effects over other lobes. Guo et al. [3] studied a 21-dimensional marker including spectrum, information theory, evoked, and connectivity features classified with DNN architecture has obtained an ACC of 92%. Sun et al. [33] extracted fuzzy entropy-based time-domain and FFT-based frequency-domain features. The 2-D images of these time-frequency domain features with a hybrid DNN model have obtained an ACC of 96.34%. Their model showed frontal and parietal lobes provided discriminable characteristics of time-domain features whereas the frontal lobe plays an important role in frequency-domain features. Vázquez et al. [34] extracted generalized partial directed coherence (GPDC) and direct directed transfer function (dDTF) features from the five EEG rhythms using autoregressive model coefficients. A feature map classified using leave-p-subjects-out cross-validation has obtained an average area under the curve of 84.67%. Chandran et al. [35] used non-linear (approximate entropy and Katz fractal dimension) and time-domain features of EEG signals. The feature map of 6790 vectors classified using the LSTM network has achieved an ACC of 99%. Baygin [36] explored the TQWT-based decomposition technique to extract twenty-five statistical moment features. Their model with ReliefF and Pearson feature selection has obtained an ACC of 99% and 83% using the *kNN* classifier. The proposed HDSS combines RVMD-based adaptive decomposition of modes, feature extraction, feature selection, and an OELM-based classifier. HDSS with six features has provided a maximum ACC of 92.93% in the second mode. The findings of Table 9 showed performance measure of the developed HDSS is superior to all the C-SOA techniques using the same dataset. The developed model is automated and does not require any predefined parameters for decomposition and classification. The HDSS model is accurate and robust as it is developed using a ten-fold cross-validation technique.

## 6. Conclusions

The HDSS in this paper has obtained superior accuracy for C-I compared to C-II and C-III. The brain captures more distinct changes in SCZ and NHC EEG signals when subject performs simultaneous auditory and motor tasks than performing separate motor and auditory tasks. The modes generated by RVMD have collectively reflected the original signal resulting in precise reconstruction with negligible RMSE. The

discriminative features of RVMD modes helped to achieve around 11% higher accuracy than VMD. The developed RVMD model has provided better analysis and perfect synthesis of nonstationary EEG signals. The third mode showed the chaotic behavior due to which higher performance for the developed HDSS is achieved. A combination of RVMD-OELM has proved superior over VMD-ELM, VMD-OELM, and RVMD-ELM by about 11%, 9%, and 2%. The proposed RVMD-OELM is robust and effective because it is evaluated using ten-fold cross-validation and obtained superior performance over existing state-of-the-art techniques. The proposed HDSS is an ideal choice for neurologists to be employed in real-time SCZ detection. In the future, we will test the model on EEG datasets of autism, attention deficit hyperactivity disorder, and Alzheimer's disease.

## Declaration of competing interest

There is no conflict of interest.

## Acknowledgments

The author would like to thank Dr. Ford and Brain Roach for providing access to the EEG dataset. The initial funding for data collection was supported by the National Institute of Mental Health (NIMH project number R01MH058262).

## References

- [1] WORLD HEALTH ORGANIZATION, <https://www.who.int/news-room/fact-sheet/detail/schizophrenia> Accessed: 21 January 2021.
- [2] S.L. Oh, J. Vicnesh, E.J. Ciaccio, R. Yuvaraj, U.R. Acharya, Deep convolutional neural network model for automated diagnosis of schizophrenia using EEG signals, *Appl. Sci.* 9 (14) (2019) 2870, <https://doi.org/10.3390/app9142870>.
- [3] Z. Guo, L. Wu, Y. Li, B. Li, Deep neural network classification of EEG data in schizophrenia, in: 2021 IEEE 10th Data Driven Control and Learning Systems Conference, DDCLS, 2021, pp. 1322–1327, <https://doi.org/10.1109/DDCLS52934.2021.9455509>.
- [4] N. Hettige, A. Bani-Fatemi, I. Sakinofsky, V. de Luca, A biopsychosocial evaluation of the risk for suicide in schizophrenia, *CNS Spectr.* 23 (2017) 1–11, <https://doi.org/10.1017/S1092852917000128>.
- [5] C. Caldwell, I. Gottesman, Schizophrenics kill themselves too: a review of risk factors for suicide, *Schizophr. Bull.* 16 (1990) 571–589, <https://doi.org/10.1093/schbul/16.4.571>.
- [6] D. Devia, R. Mayol-Troncoso, J. Parrini, G. Orellana, A. Ruiz, P.E. Maldonado, J. I. Egana, EEG classification during scene free-viewing for schizophrenia detection, *IEEE Trans. Neural Syst. Rehabil. Eng.* 27 (6) (2019) 1193–1199, <https://doi.org/10.1109/TNSRE.2019.2913799>.
- [7] N. Kannathal, U.R. Acharya, C. Lim, P. Sadasivan, Characterization of EEG-A comparative study, *Comput. Methods Progr. Biomed.* 80 (1) (2005) 17–23, <https://doi.org/10.1016/j.cmpb.2005.06.005>.
- [8] P. Sawangjai, S. Hompoonsup, P. Leelaarporn, S. Kongwudhikunakorn, T. Wilaprasitpon, Consumer grade EEG measuring sensors as research tools: a review, *IEEE Sensor. J.* 20 (8) (2020) 3996–4024.
- [9] U.R. Acharya, S. Vinitha Sree, G. Swapna, R.J. Martis, J.S. Suri, Automated EEG analysis of epilepsy: a review, *Knowl. Base Syst.* 45 (2013) 147–165, <https://doi.org/10.1016/j.knosys.2013.02.014>.
- [10] S.D. Puthankattil, P. Joseph, U.R. Acharya, C. Lim, EEG signal analysis: a survey, *J. Med. Syst.* 34 (2010) 195–212, <https://doi.org/10.1007/s10916-008-9231-z>.
- [11] S.H. Na, S.-H. Jin, S.Y. Kim, B.-J. Ham, EEG in schizophrenic patients: mutual information analysis, *Clin. Neurophysiol.* 113 (12) (2002) 1954–1960, [https://doi.org/10.1016/S1388-2457\(02\)00197-9](https://doi.org/10.1016/S1388-2457(02)00197-9).
- [12] L. Zhang, EEG signals classification using machine learning for the identification and diagnosis of schizophrenia, in: 2019 41st Annual International Conference of the IEEE Engineering in Medicine and Biology Society, EMBC, 2019, pp. 4521–4524, <https://doi.org/10.1109/EMBC.2019.8857946>.
- [13] M. Sabeti, S. Katebi, R. Boostani, Entropy and complexity measures for EEG signal classification of schizophrenic and control participants, *Artif. Intell. Med.* 47 (3) (2009) 263–274, <https://doi.org/10.1016/j.artmed.2009.03.003>.
- [14] Ying-jie Li, Fei-yan Fan, Classification of schizophrenia and depression by EEG with amns, in: 2005 IEEE Engineering in Medicine and Biology 27th Annual Conference, 2005, pp. 2679–2682, <https://doi.org/10.1109/IEMBS.2005.1617022>.
- [15] M. Sabeti, S. Katebi, R. Boostani, G. Price, A new approach for EEG signal classification of schizophrenic and control participants, *Expert Syst. Appl.* 38 (3) (2011) 2063–2071, <https://doi.org/10.1016/j.eswa.2010.07.145>.
- [16] M. Shim, H.-J. Hwang, D.-W. Kim, S.-H. Lee, C.-H. Im, Machine-learning-based diagnosis of schizophrenia using combined sensor-level and source-level eeg features, *Schizophr. Res.* 176 (2) (2016) 314–319, <https://doi.org/10.1016/j.schres.2016.05.007>.

- [17] J. Sui, E. Castro, H. He, D. Bridwell, Y. Du, G.D. Pearlson, T. Jiang, V.D. Calhoun, Combination of fMRI-SMRI-EEG data improves discrimination of schizophrenia patients by ensemble feature selection, in: 2014 36th Annual International Conference of the IEEE Engineering in Medicine and Biology Society, 2014, pp. 3889–3892, <https://doi.org/10.1109/EMBC.2014.6944473>.
- [18] Z. Dvey-Aharon, N. Fogelson, A. Peled, N. Intrator, Schizophrenia detection and classification by advanced analysis of EEG recordings using a single electrode approach, *PLoS One* 10 (4) (2015) 1–12, <https://doi.org/10.1371/journal.pone.0123033>.
- [19] C. Phang, C. Ting, S.B. Samdin, H. Ombao, Classification of EEG-based effective brain connectivity in schizophrenia using deep neural networks, in: 2019 9th International IEEE/EMBS Conference on Neural Engineering, NER, 2019, pp. 401–406, <https://doi.org/10.1109/NER.2019.8717087>.
- [20] A. Bachiller, A. Lubeiro, I. Díez, V. Suazo, C. Domínguez, J. Blanco, M. Ayuso, R. Hornero, J. Poza, V. Molina, Decreased entropy modulation of EEG response to novelty and relevance in schizophrenia during a P300 task, *Eur. Arch. Psychiatr. Clin. Neurosci.* (2014) 525–535, <https://doi.org/10.1007/s00406-014-0525-5>.
- [21] S. Nasehi, H. Pourghassem, A novel effective feature selection algorithm based on S-PCA and wavelet transform features in EEG signal classification, in: 2011 IEEE 3rd International Conference on Communication Software and Networks, 2011, pp. 114–117, <https://doi.org/10.1109/ICCSN.2011.6014686>.
- [22] S.A. Akar, S. Kara, F. Latifoglu, V. Bilgiç, Wavelet-welch methodology for analysis of EEG signals of schizophrenia patients, in: 2012 Cairo International Biomedical Engineering Conference, CIBEC, 2012, pp. 6–9, <https://doi.org/10.1109/CIBEC.2012.6473311>.
- [23] S. Siuly, S.K. Khare, V. Bajaj, H. Wang, Y. Zhang, A computerized method for automatic detection of schizophrenia using EEG signals, *IEEE Trans. Neural Syst. Rehabil. Eng.* 28 (11) (2020) 2390–2400, <https://doi.org/10.1109/TNSRE.2020.3022715>.
- [24] P.T. Krishnan, A.N. Joseph Raj, P. Balasubramanian, Y. Chen, Schizophrenia detection using multivariate empirical mode decomposition and entropy measures from multichannel EEG signal, *Biocybern. Biomed. Eng.* 40 (3) (2020) 1124–1139, <https://doi.org/10.1016/j.bbe.2020.05.008>.
- [25] M. Sharma, U. R. Acharya, Automated Detection of Schizophrenia Using Optimal Wavelet-Based L 1 Norm Features Extracted from Single-Channel EEG, *Cognitive Neurodynamics* doi:10.1007/s11571-020-09655-w.
- [26] S.K. Khare, V. Bajaj, S. Siuly, G.R. Sinha, Classification of schizophrenia patients through empirical wavelet transformation using electroencephalogram signals, in: Modelling and Analysis of Active Biopotential Signals in Healthcare, vol. 1, IOP Publishing, 2020, pp. 2053–2563, <https://doi.org/10.1088/978-0-7503-3279-8ch1>, 1–1 to 2–26.
- [27] H. Akbari, S. Ghofrani, P. Zakalvand, M. Tariq Sadiq, Schizophrenia recognition based on the phase space dynamic of EEG signals and graphical features, *Biomed. Signal Process Control* 69 (2021) 102917, <https://doi.org/10.1016/j.bspc.2021.102917>.
- [28] V. Knott, C. Mahoney, A. Labelle, C. Ripley, P. Cavazzoni, B. Jones, Event-related potentials in schizophrenic patients during a degraded stimulus version of the visual continuous performance task, *Schizophr. Res.* 35 (3) (1999) 263–278.
- [29] J.A. Taylor, N. Matthews, P.T. Michie, M.J. Rosa, M.I. Garrido, Auditory prediction errors as individual biomarkers of schizophrenia, *Neuroimage: Clinic* 15 (2017) 264–273.
- [30] S.K. Khare, V. Bajaj, U.R. Acharya, SPWVD-CNN for automated detection of schizophrenia patients using EEG signals, *IEEE Trans. Instrument. Meas.* 70 (2021) 1–9, <https://doi.org/10.1109/TIM.2021.3070608>.
- [31] D. Iyer, N.N. Boutros, G. Zouridakis, Single-trial analysis of auditory evoked potentials improves separation of normal and schizophrenia subjects, *Clin. Neurophysiol.* 123 (9) (2012) 1810–1820.
- [32] A.H. Neuhaus, F.C. Popescu, C. Grozea, E. Hahn, C. Hahn, C. Opgen-Rhein, C. Urbanek, M. Dettling, Single-subject classification of schizophrenia by event-related potentials during selective attention, *Neuroimage* 55 (2) (2011) 514–521.
- [33] J. Sun, C. Rui, M. Zhou, M. Hussain, B. Wang, J. Xue, J. Xiang, A hybrid deep neural network for classification of schizophrenia using EEG data, *Sci. Rep.* 11. doi: 10.1038/s41598-021-83350-6..
- [34] M. Vázquez, A. Maghsoudi, I. Mariño, An interpretable machine learning method for the detection of schizophrenia using EEG signals, *Front. Syst. Neurosci.* 15 (2021) 1–11, <https://doi.org/10.3389/fnsys.2021.652662>.
- [35] A. Nikhil Chandran, K. Sreekumar, D.P. Subha, EEG-based automated detection of schizophrenia using long short-term memory (LSTM) network, in: S. Patnaik, X.-S. Yang, I.K. Sethi (Eds.), *Advances in Machine Learning and Computational Intelligence*, Springer Singapore, Singapore, 2021, pp. 229–236.
- [36] M. Baygin, An accurate automated schizophrenia detection using tqwt and statistical moment based feature extraction, *Biomed. Signal Process Control* 68 (2021) 102777, <https://doi.org/10.1016/j.bspc.2021.102777>.
- [37] S.K. Khare, V. Bajaj, Entropy based drowsiness detection using adaptive variational mode decomposition, *IEEE Sensor. J.* (2020), <https://doi.org/10.1109/JSEN.2020.3038440>, 1–1.
- [38] S.K. Khare, V. Bajaj, An evolutionary optimized variational mode decomposition for emotion recognition, *IEEE Sensor. J.* 21 (2) (2021) 2035–2042, <https://doi.org/10.1109/JSEN.2020.3020915>.
- [39] S.K. Khare, V. Bajaj, A facile and flexible motor imagery classification using electroencephalogram signals, *Comput. Methods Progr. Biomed.* 197 (2020) 105722, <https://doi.org/10.1016/j.cmpb.2020.105722>.
- [40] J.M. Ford, V.A. Palzes, B.J. Roach, D.H. Mathalon, Did I do that? Abnormal predictive processes in schizophrenia when button pressing to deliver a tone, *Schizophr. Bull.* 40 (4) (2013) 804–812, <https://doi.org/10.1093/schbul/sbt072>.
- [41] <https://www.kaggle.com/broach/button-tone-sz>, Access 22 Jun 2020.
- [42] K. Dragomireskiy, D. Zosso, Variational mode decomposition, *IEEE Trans. Signal Process.* 62 (3) (2014) 531–544, <https://doi.org/10.1109/TSP.2013.2288675>.
- [43] J. Lian, Z. Liu, H. Wang, X. Dong, Adaptive variational mode decomposition method for signal processing based on mode characteristic, *Mech. Syst. Signal Process.* 107 (2018) 53–77, <https://doi.org/10.1016/j.ymssp.2018.01.019>.
- [44] Z. Wang, G. He, W. Du, J. Zhou, X. Han, J. Wang, H. He, X. Guo, J. Wang, Y. Kou, Application of parameter optimized variational mode decomposition method in fault diagnosis of gearbox, *IEEE Access* 7 (2019) 44871–44882, <https://doi.org/10.1109/ACCESS.2019.2909300>.
- [45] S. Mirjalili, A. Lewis, The whale optimization algorithm, *Adv. Eng. Software* 95 (2016) 51–67, <https://doi.org/10.1016/j.advengsoft.2016.01.008>.
- [46] A. Phinyomark, P. Phukpattaranont, C. Limksakul, Feature reduction and selection for EMG signal classification, *Expert Syst. Appl.* 39 (8) (2012) 7420–7431, <https://doi.org/10.1016/j.eswa.2012.01.102>.
- [47] G.-B. Huang, Q.-Y. Zhu, C.-K. Siew, Extreme learning machine: theory and applications, *Neurocomputing* 70 (1) (2006) 489–501, <https://doi.org/10.1016/j.neucom.2005.12.126>, neural Networks.



Smith K. Khare is a research scholar in Indian Institute of Information Technology, Design and Manufacturing, Jabalpur, India. Mr. Smith has authored/co-authored 25 publications in high impact factor, peer-reviewed journals like IEEE Transactions, Elsevier, etc. He has authored in 8 book chapters and 2 paper in international conference. He is serving as a reviewer in IEEE, Elsevier and several other reputed journals. His research interests include biomedical signal processing, pattern recognition, brain-computer interface, machine learning, artificial intelligence in healthcare, and deep neural networks.



Varun Bajaj (PhD, SMIEE20) is working as a Associate Professor in the discipline of Electronics and Communication Engineering, at Indian Institute of Information Technology, Design and Manufacturing (IIITDM) Jabalpur, India since July 2021. He worked as Assistant Professor in IIITDM Jabalpur from March 2014 to July 2021. He also worked as a visiting faculty in IIITDM Jabalpur from September 2013 to March 2014. He worked as Assistant Professor at Department of Electronics and Instrumentation, Shri Vaishnav Institute of Technology and Science, Indore, India during 2009–2010. He received his Ph.D. degree in the Discipline of Electrical Engineering, at Indian Institute of Technology Indore, India in 2014. He received M.Tech. Degree with Honors in Microelectronics and VLSI design from Shri Govindram Seksaria Institute of Technology & Science, Indore, India in 2009, B.E. degree in Electronics and Communication Engineering from Rajiv Gandhi Technological University, Bhopal, India in 2006.

He is an Associate Editor of IEEE Sensor Journal and Subject Editor-in-Chief of IET Electronics Letters. He served as a Subject Editor of IET Electronics Letters from Nov-2018 to June 2020. He is Senior Member IEEE June 2020, MIEEE 16–20, and also contributing as active technical reviewer of leading International journals of IEEE, IET, and Elsevier, etc. He has authored more than 110 research papers in various reputed international journals/conferences like IEEE Transactions, Elsevier, Springer, IOP etc. He has edited Books in IOP, CRC Publisher. The citation impact of his publications is around 3251 citations, h index of 29, and i10 index of 72 (Google Scholar Nov 2021). He has guided seven (04 completed and 3 In process) PhD Scholars, 7 M. Tech. Scholars. He is a recipient of various reputed national and international awards. His research interests include biomedical signal processing, image processing, time-frequency analysis, and computer-aided medical diagnosis.